



This is a repository copy of *A unified potential drop calibration function for common crack growth specimens*.

White Rose Research Online URL for this paper:  
<http://eprints.whiterose.ac.uk/131428/>

Version: Published Version

---

**Article:**

Tarnowski, K.M., Nikbin, K.M., Dean, D.W. et al. (1 more author) (2018) A unified potential drop calibration function for common crack growth specimens. *Experimental Mechanics*, 58 (6). pp. 1003-1013. ISSN 0014-4851

<https://doi.org/10.1007/s11340-018-0398-z>

---

© The Author(s) 2018. This article is distributed under the terms of the Creative Commons Attribution 4.0 International License (<http://creativecommons.org/licenses/by/4.0/>), which permits unrestricted use, distribution, and reproduction in any medium, provided you give appropriate credit to the original author(s) and the source, provide a link to the Creative Commons license, and indicate if changes were made.

**Reuse**

This article is distributed under the terms of the Creative Commons Attribution (CC BY) licence. This licence allows you to distribute, remix, tweak, and build upon the work, even commercially, as long as you credit the authors for the original work. More information and the full terms of the licence here:  
<https://creativecommons.org/licenses/>

**Takedown**

If you consider content in White Rose Research Online to be in breach of UK law, please notify us by emailing [eprints@whiterose.ac.uk](mailto:eprints@whiterose.ac.uk) including the URL of the record and the reason for the withdrawal request.



[eprints@whiterose.ac.uk](mailto:eprints@whiterose.ac.uk)  
<https://eprints.whiterose.ac.uk/>

# *A Unified Potential Drop Calibration Function for Common Crack Growth Specimens*

**K.M. Tarnowski, K.M. Nikbin,  
D.W. Dean & C.M. Davies**

**Experimental Mechanics**  
An International Journal

ISSN 0014-4851

Exp Mech  
DOI 10.1007/s11340-018-0398-z



 Springer

**Your article is published under the Creative Commons Attribution license which allows users to read, copy, distribute and make derivative works, as long as the author of the original work is cited. You may self-archive this article on your own website, an institutional repository or funder's repository and make it publicly available immediately.**



# A Unified Potential Drop Calibration Function for Common Crack Growth Specimens

K.M. Tarnowski<sup>1</sup> · K.M. Nikbin<sup>1</sup> · D.W. Dean<sup>2</sup> · C.M. Davies<sup>1</sup>

Received: 17 February 2017 / Accepted: 30 April 2018  
© The Author(s) 2018

## Abstract

Calibration functions, used to determine crack extension from potential drop measurements, are not readily available for many common crack growth specimen types. This restricts testing to a limited number of specimen types, typically resulting in overly conservative material properties being used in residual life assessments. This paper presents a unified calibration function which can be applied to all common crack growth specimen types, mitigating this problem and avoiding the significant costs associated with the current conservative approach. Using finite element analysis, it has been demonstrated that Johnson's calibration function can be applied to the seven most common crack growth specimen types: C(T), SEN(T), SEN(B), M(T), DEN(T), CS(T) and DC(T). A parametric study has been used to determine the optimum configuration of electrical current inputs and PD probes. Using the suggested configurations, the error in the measurement of crack extension is <6% for all specimen types, which is relatively small compared to other sources of error commonly associated with the potential drop technique.

**Keywords** Crack growth · Potential drop · Calibration function · Finite element analysis

## Nomenclature

### Symbols

$\Delta a$	Instantaneous crack extension
$a$	Instantaneous crack length
$a_f$	Final crack length
$a_0$	Initial crack length
$B$	Specimen thickness
$F_y$	Correction factor to account for variations in PD probe location
$V$	Potential drop corresponding to the instantaneous crack length
$V_0$	Potential drop corresponding to the initial crack length
$V_r$	Potential drop corresponding to a reference crack length
$W$	Specimen width
$y$	Perpendicular distance between the crack plane and the PD probes
$y_l$	Perpendicular distance between the crack plane and the current injection point

$\alpha$	Angle defining the current injection location in a DC(T) specimen
$\theta$	Angle defining the current injection location in a CS(T) specimen

### Acronyms

CS(T)	C-Shaped Tension
C(T)	Compact Tension
DC	Direct Current
DCPD	Direct Current Potential Drop
DEN(T)	Double Edge-Notch Tension
DC (T)	Disc-shaped Compact Tension
EDM	Electrical Discharge Machined
FE	Finite Element
LLD	Load-Line Displacement
M(T)	Middle Tension
PD	Potential Drop
SEN(B)	Single Edge-Notch Bend
SEN(T)	Single Edge-Notch Tension

✉ K.M. Tarnowski  
k.tarnowski@sheffield.ac.uk

<sup>1</sup> Department of Mechanical Engineering, Imperial College London, London SW7 2AZ, UK

<sup>2</sup> EDF Energy, Barnett Way, Barnwood, Gloucester GL4 3RS, UK

## Introduction

Direct Current Potential Drop (DCPD) is one of the most common techniques employed for measuring crack extension in the laboratory. It works on the principle that a constant



current flowing through a specimen containing a crack generates an electrical field which is sensitive to changes in geometry, in particular crack extension. As the crack grows the PD, measured between two probes located either side of the crack, will increase. Using a suitable calibration function, this can be correlated with crack extension [1].

The seven most common crack growth specimen types are:

- Compact Tension, C(T),
- Middle Tension, M(T),
- Single Edge-Notched Tension, SEN(T),
- Single Edge-Notched Bend, SEN(B),
- Double Edge-Notched Tension, DEN(T),
- C-Shaped Tension, CS(T),
- Disc-shaped Compact Tension, DC(T).

Calibration functions are only readily available in the literature for a few of these specimen geometries, e.g. [2]. This can prevent crack growth tests from using the specimen type that is most representative of the component for which the test is being performed. A direct consequence of this is that high constraint bend specimens such as C(T) or SEN(B) are typically used to obtain conservative material properties, but this results in an underestimation of the residual life of the component and potentially significant economic, social and environmental costs associated with unnecessary repair or replacement work. To avoid this, it is vital that calibration functions are readily available for all common specimen types used for crack growth testing.

The aim of this investigation is to determine whether a single ‘unified’ calibration function can be applied to all of the crack growth specimen types listed above. This approach would not only permit testing to be performed using the most representative specimen type, but would also be ideal for standardisation where it is often not desirable to publish numerous individual calibration functions.

The formula derived by Johnson [3] is probably the most common calibration function and will be used as the basis for this investigation. Johnson’s calibration function is discussed in the following sub-section followed by a review of previous efforts to apply this calibration function to a range of specimen types.

### Johnson’s Calibration Function

Johnson [3] used analytical methods to derive an exact calibration function for the M(T) specimen geometry shown in Fig. 1. The derivation was based on the following assumptions: a crack of infinitesimal width; a uniform current injected remote from the crack; PD probes along the centre-line of the specimen, equidistant from the crack. Johnson’s calibration function is provided in equation (1) where  $V$  is the PD

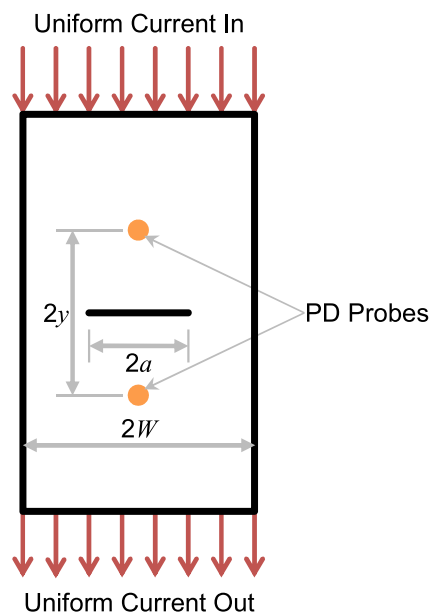


Fig. 1 M(T) specimen geometry assumed in the derivation of equation (1) [3]

corresponding to the instantaneous crack length,  $a$ , and  $V_0$  is the PD corresponding to the initial crack length,  $a_0$ .

$$\frac{a}{W} = \frac{2}{\pi} \cos^{-1} \left[ \frac{\cosh\left(\frac{\pi y}{2W}\right)}{\cosh\left(\frac{V}{V_0} \cosh^{-1}\left\{\frac{\cosh\left(\frac{\pi y}{2W}\right)}{\cos\left(\frac{\pi a_0}{2W}\right)}\right\}\right)} \right] \quad (1)$$

One of the main advantages of equation (1) is its general form which means it can be directly applied to any initial crack length. Most other calibration functions, which are usually derived by empirical or numerical methods, require a reference PD,  $V_r$ , which corresponds to a specific crack length. A typical example is equation (2) which applies to a C(T) specimen where the reference PD corresponds to  $a = 0.241 W$  [2].

$$\frac{a}{W} = -0.5051 + 0.8857\left(\frac{V}{V_r}\right) - 0.1398\left(\frac{V}{V_r}\right)^2 + 0.0002398\left(\frac{V}{V_r}\right)^3 \quad (2)$$

For tests where the initial crack length is  $0.241 W$ , the reference PD,  $V_r$ , can be measured at the start of the test, but for tests with any other initial crack length, an additional step is required whereby the value of  $V_r$  is calculated from the initial crack length,  $a_0$ , and the corresponding PD,  $V_0$ , using the inverted version of equation (2) provided in equation (3).

$$\frac{V_0}{V_r} = 0.5766 + 1.9169\left(\frac{a_0}{W}\right) - 1.0712\left(\frac{a_0}{W}\right)^2 + 1.6898\left(\frac{a_0}{W}\right)^3 \quad (3)$$

This increases the complexity of the calculation required to determine crack length from PD measurements. For reasons of relative simplicity and versatility, the calibration function derived by Johnson will therefore be used as the basis for the following investigation.

### The Application of Johnson's Calibration Function to a Range of Specimen Types

Schwalbe and Hellman [4] observed that the M(T) specimen in Fig. 1 is geometrically equivalent to two mirrored SEN specimens, where SEN refers to both SEN(T) and SEN(B). This is shown schematically in Fig. 2(a). Although SEN(T) and SEN(B) specimens are not mechanically equivalent, they are identical from a calibration point of view. Similar to a M(T) specimen, a DEN(T) is also equivalent to two mirrored SEN specimens [5], as shown in Fig. 2(b). It follows that equation (1) is an exact solution for four of the most common specimen types (namely M(T), SEN(T), SEN(B) and DEN(T)), as long as the current distribution is uniform and the PD is monitored at locations geometrically equivalent to those shown in Fig. 1. Schwalbe and Hellman [4] also observed that a C(T) specimen is effectively a short SEN, as shown in Fig. 2(c). Despite the obvious geometric differences (pin holes, increased width and the reduced height), equation (1) is often successfully applied to C(T) specimens e.g. [6].

Of the remaining geometries considered in this study, a DC(T) is geometrically similar to a C(T) specimen, and a CS(T) is geometrically similar to a SEN specimen. It is therefore likely that this equation (1) may be applied to all seven specimen geometries considered here without introducing significant errors in the measurement of crack extension. This makes it an ideal candidate for a 'unified calibration function'.

Gilbey and Pearson [7] derived a more general form of equation (1) which incorporates a non-uniform current injected

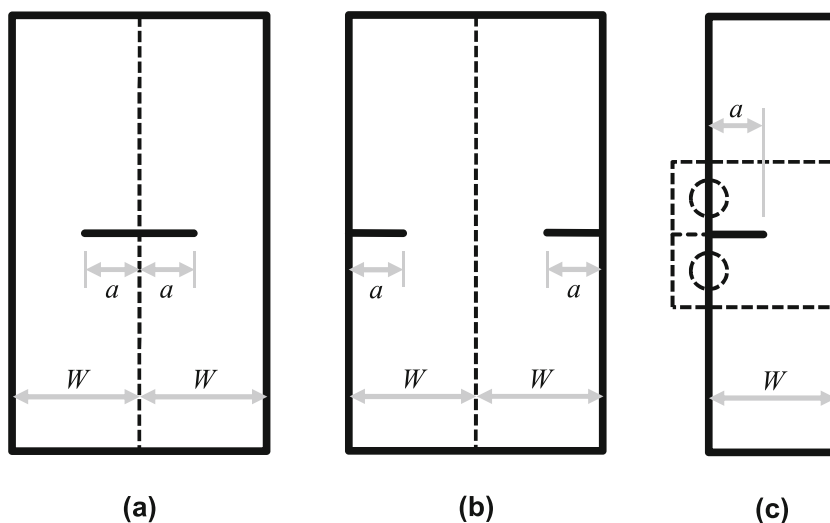
at a point. For specimens such as SEN(T), SEN(B), M(T) and DEN(T), where the current is typically injected remote from the crack, this calibration function tends towards equation (1) [8], but for compact specimens such as C(T) and DC(T), it is likely to be able to capture the relationship between PD and crack length more accurately. Despite this, the calibration function derived by Gilbey and Pearson will not be considered further because it is extremely complex. It is therefore not aligned with the aim of this paper which is to provide a simple calibration function suitable for a wide range of specimens.

In this investigation, the work performed by Schwalbe and Hellman [4] will be extended to include all of the specimen types listed above. For each geometry the PD configuration (current injection and PD probe location) will be optimised to minimise the error in the prediction of crack extension using Johnson's calibration function. This will be performed using Finite Element (FE) analysis because it is a simple, accurate and fast tool for deriving calibration functions [9] which allows the influence of the PD configuration to be assessed in isolation by providing precise control of all other variables that can influence the PD response, e.g. crack length, crack shape, specimen geometry, current, temperature, etc. The same level of control cannot be obtained experimentally. For these reasons, FE analysis has been used for many previous PD optimisation studies, e.g. [10–12].

### Methodology

A series of electrical FE analyses have been performed to determine the optimum PD configurations for determining crack extension with Johnson's calibration function for the seven most common crack growth specimen types. An overview of the methodology implemented in this study is outlined here and shown schematically in Fig. 3:

**Fig. 2** Geometric similarities between (a) a M(T) and two SEN specimens; (b) a DEN(T) and two SEN specimens; (c) a SEN and a C(T) specimen





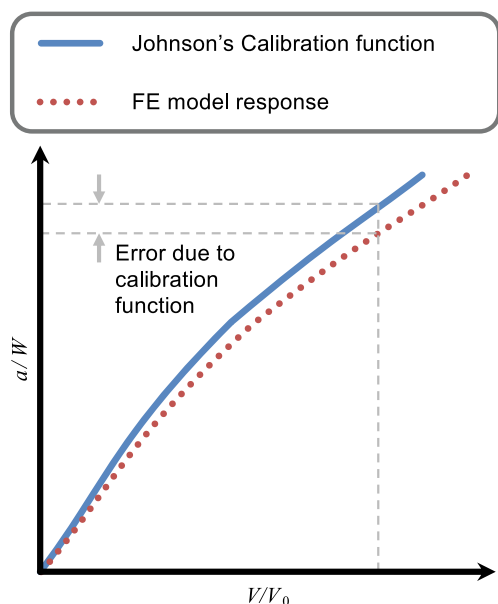


**Fig. 3** Schematic representation of the error associated with the application of Johnson's calibration function

1. For each specimen type a 2D FE model was generated.
2. Each model was used to perform a parametric study to determine the relationship between PD and crack length for a range PD configurations by increasing the crack length in a series of small increments.
3. The PD data from each analysis was used to predict the crack extension using Johnson's calibration function for each increment of crack length.
4. The crack extension predicted from the PD data was compared with the actual crack extension in the model to determine the error due to the application of Johnson's calibration function.
5. For each specimen type the PD configuration that corresponded to the smallest error was identified.

General details of the specimen geometries, PD configurations, and FE modelling approach are provided in the following sub-sections. Specific details of the individual analyses are provided with the results for each specimen type.

### Specimen Geometries

The specimen geometries considered in this study are:

- Compact Tension, C(T),
- Middle Tension, M(T),
- Single Edge-Notched Tension, SEN(T),
- Single Edge-Notched Bend, SEN(B),
- Double Edge-Notched Tension, DEN(T),
- C-Shaped Tension, CS(T),
- Disc-shaped Compact Tension, DC(T).

The minimum initial crack length used in C(T), SEN(B) and DC(T) specimens is typically  $0.45 W$  [6, 13] whereas in M(T), SEN(T), DEN(T) and CS(T) specimens it is often much smaller and can be as little as  $0.10 W$ . For all specimen types, if the remaining ligament becomes very small (typically  $a > 0.70 W$ ), gross plasticity can occur and the specimen no longer represents a cracked structure. In this study, the PD configurations for C(T), SEN(B) and DC(T) specimens have been optimised for crack lengths in the range  $0.45 \leq a/W \leq 0.70$ , whilst the PD configurations for M(T), SEN(T), DEN(T) and CS(T) specimens have been optimised for crack lengths in the range  $0.10 \leq a/W \leq 0.70$ .

Johnson's calibration function is derived for a specimen with a crack of infinitesimal width, as shown in Fig. 1, but specimens used in real crack growth tests often include a starter notch. The size and shape of this notch depends on the type of test being performed. For example, if load-line displacement (LLD) measurements are required then a large notch is often necessary to accommodate an extensometer. Rather than prescribing a specific notch geometry, most crack growth standards provide a maximum geometric envelope that the notch must fit within, e.g. [13]. This can have significant implications when trying to use a single calibration function for all possible notch geometries because the accuracy of the crack extension measurement depends on the geometry of the notch and the length of the pre-crack ahead of the notch [1]. For consistency, all of the specimens considered in this study have been modelled a crack of infinitesimal width, similar to the original derivation of Johnson's calibration function, i.e. no starter notch. The influence of a started notch has been considered separately in a sensitivity study performed on the C(T) specimen; the most common crack growth specimen type. This sensitivity study is presented in "C(T) Specimen" section.

### PD Configurations

The optimum PD probe location is across the crack mouth and close to the plane of the crack, as identified in multiple studies, e.g. [10, 14]. At this location the measurement is both sensitive and repeatable, i.e. the PD is sensitive to crack growth, but not to slight misplacement of the probes. The probe location used in the derivation of Johnson's calibration function is also across the crack mouth, but the distance from the crack plane,  $y$ , is a variable. To ensure an optimum PD configuration is considered in this investigation, a realistically achievable minimum value of  $y$  has been used for all specimens. For specimens modelled without a starter notch, a value of  $y$  of  $0.08 W$  has been used consistently. This is a distance of 2.0 mm from the crack plane assuming a specimen width,  $W$ , of 25 mm, which is a common specimen size, e.g. [6]. For the starter notch sensitivity study, larger values of  $y$  were required because the material close to the crack plane was removed to

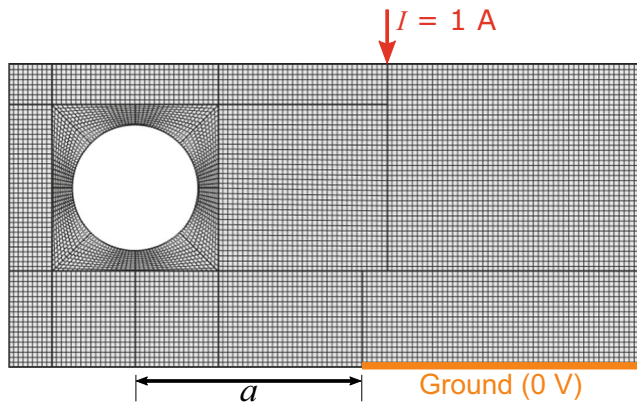


Fig. 4 FE mesh for a C(T) specimen

form the notch. The exact PD probe locations used in this sensitivity study are provided in “C(T) Specimen” section.

Johnson’s calibration function was derived for a uniform current distribution, as shown in Fig. 1, but in most crack growth tests the current is injected at a point via a spot-weld or threaded connection. A point current source is more representative of this configuration and has been considered throughout this investigation. Some experimentalists have attempted to apply a distributed current to crack growth specimens, e.g. via a copper sheet soldered, brazed or screwed to the specimen, but this is much less common and inconsistencies in the contact between the specimen and the copper sheet can introduce uncertainty in the measurement [14, 15]. Details of the exact PD configurations are provided with the results for each specimen type.

### Finite Element Modelling

For each specimen type a 2D FE model was developed using COMSOL [16]. A typical model is shown in Fig. 4 for a C(T) specimen. Only half the specimen was modelled exploiting the symmetry about the crack plane. Each model was meshed

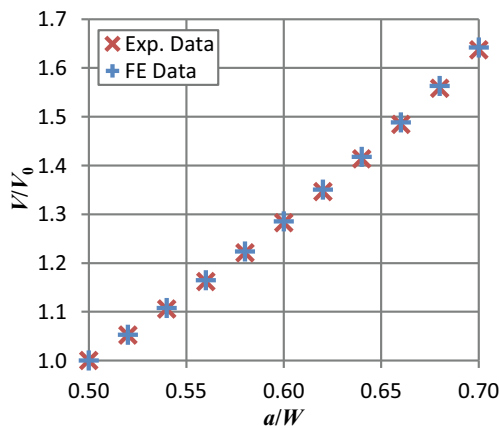


Fig. 5 Validation of the FE modelling methodology by comparison of normalised PD vs. crack length predicted from a 2D FE model with experimental data obtained by incremental EDM slitting

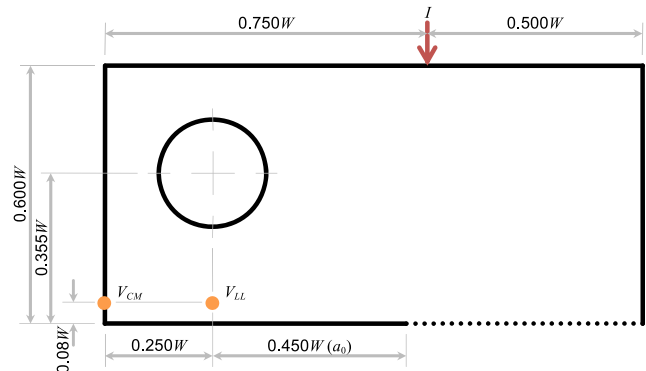


Fig. 6 Half C(T) specimen, remaining ligament identified by the dotted line

using linear quadrilateral elements with an approximate element size of  $0.01 W$ . A mesh refinement study was performed which demonstrated convergence for this element size.

The boundary conditions applied to a typical analysis are also shown in Fig. 4. A unit current was applied to a single node and an electrical ground (0 V) was applied to the ligament ahead of the crack. All other surfaces were assumed to be perfectly insulated. Crack growth was simulated by reducing the length of the region along which the electrical ground boundary condition was applied. This was done in small increments and for each increment the PD was monitored at the selected probe location.

Two preliminary FE analysis were performed to validate the modelling procedure. The first was performed on a 2D model of the exact M(T) specimen geometry and PD configuration shown in Fig. 1 for  $0.10 \leq a/W \leq 0.70$ . Johnson’s calibration function, was used to predict crack extension from the PD measurements obtained from the analysis and this was compared with the actual crack extension in the model. The predicted crack extension was consistently within 0.2% of the actual crack extension providing confidence in the general modelling procedure.

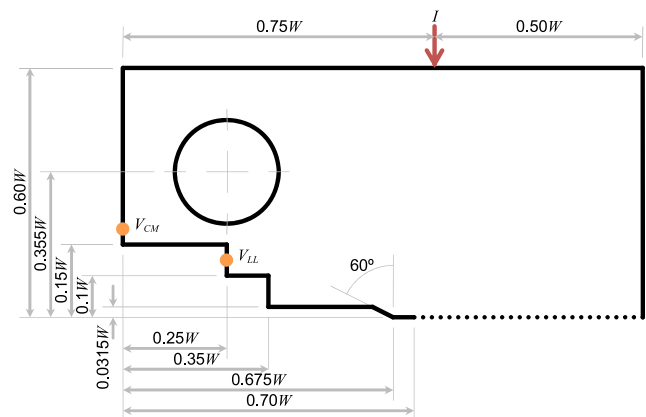
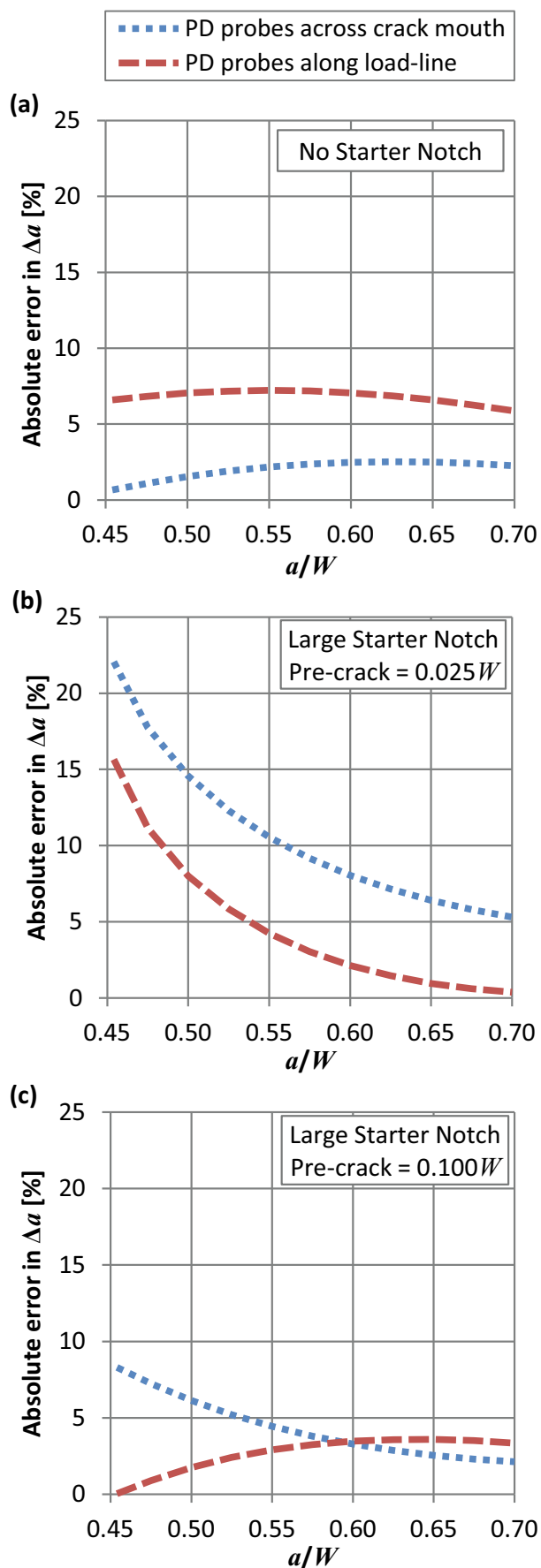


Fig. 7 Half C(T) specimen, including maximum allowable starter notch from ASTM E1820 [13], the remaining ligament identified by the dotted line





◀ Fig. 8 Absolute error in the measurement of crack extension for a C(T) specimen with (a) no notch; (b) a large notch with a pre-crack of  $0.025W$ , (c) a large notch with a pre-crack of  $0.100W$

The second preliminary analysis compared the results of a 2D and a 3D FE model of a C(T) specimen for  $0.45 \leq a/W \leq 0.70$ . A typical specimen thickness,  $B$ , of  $0.5W$  was assumed in the 3D model. The C(T) specimen geometry was selected for this comparison because it is most likely to be susceptible to any 3D effects due to its compact geometry. Johnson's calibration function, was used to predict the crack extension from the PD measurements obtained from both analyses. The difference between the crack extension predicted for the two models was consistently  $<0.1\%$  providing confidence in the use of 2D FE models throughout this investigation.

To further validate the modelling procedure the results from a 2D FE analysis of a C(T) specimen were directly compared to experimental data obtained from a real specimen ( $W = 50$  mm,  $B = 25$  mm). A  $0.3$  mm wide electrical discharge machined (EDM) slot was used to simulate crack growth in the real specimen. This was cut in increments of  $0.02W$  ( $1.0$  mm) from  $0.50 \leq a/W \leq 0.70$ . The results from the FE analysis are compared the experimental data in Fig. 5 with excellent agreement providing further confidence in the modelling procedure.

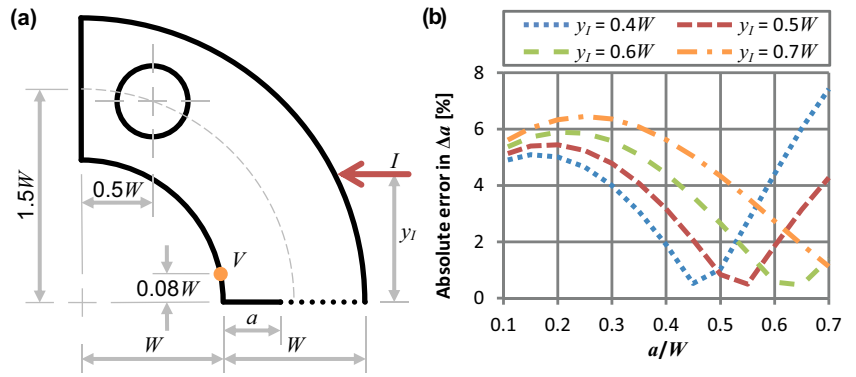
## Results & Discussion

### C(T) Specimen

The C(T) specimen geometry considered in this investigation, including the PD configurations, is shown in Fig. 6. Two PD probe locations have been considered, one across the crack mouth,  $V_{CM}$ , and the other along the load-line,  $V_{LL}$ . The combination of the current injection location,  $I$ , and the PD probe location  $V_{CM}$  was identified by Schwalbe and Hellman [4] as a configuration which produces a PD response similar to Johnson's calibration function. The alternative PD probe location along the load-line was not considered by Schwalbe and Hellman but is included here because it is more representative of the location used by Johnson in the derivation of equation (1) (see Fig. 2(c)). Another benefit of locating the PD probes along the load-line is that this configuration is less susceptible to errors related to large strains around the pin holes. It is therefore more suited to applications such as fracture toughness testing where a combination of a ductile material and a large starter notch can result in significant plastic strains in this location [17].

Sensitivity studies have also been performed on the C(T) specimen geometry to investigate the influence of the starter notch and the length of the pre-crack ahead of the starter notch. Two additional analyses were performed:

**Fig. 9** (a) CS(T) specimen geometry; (b) corresponding absolute error in the measurement of crack extension for different PD configurations



1. A C(T) specimen including the maximum allowable notch from ASTM E1820 [13]. This includes a  $0.05B$  long pre-crack ahead of the notch which, for a typical specimen where  $B = W/2$ , is  $0.025 W$ . This geometry is shown in Fig. 7.
2. A C(T) specimen including a modified version of the maximum allowable notch from ASTM E1820 [13] where the length of the pre-crack ahead of the notch was increased to  $0.1 W$ . The length of the notch was reduced accordingly so the initial crack length remained  $0.45 W$ . It has been shown that increasing the length of the pre-crack to a  $0.1 W$  significantly reduces the influence of the starter notch on the PD response [1].

For both of these analyses, the PD probe locations shown in Fig. 6 were not possible due to the removal of the notch material so slightly different locations were considered. For the PD probes across the crack mouth,  $y = 0.175 W$ , whilst for the PD probes along the load-line,  $y = 0.125 W$ . When calculating the crack extension using Johnson’s calibration function, the appropriate value of  $y$  was used in equation (1).

The absolute error in the measurement of crack extension when using Johnson’s calibration function is shown for both PD probe locations in Fig. 8. Figure 8(a) corresponds to a specimen without a starter notch i.e. just a pre-crack of infinitesimal width. Figure 8(b) corresponds to a specimen with a large starter notch and a pre-crack of  $0.025 W$  ahead of the notch. Figure 8(c) corresponds to a

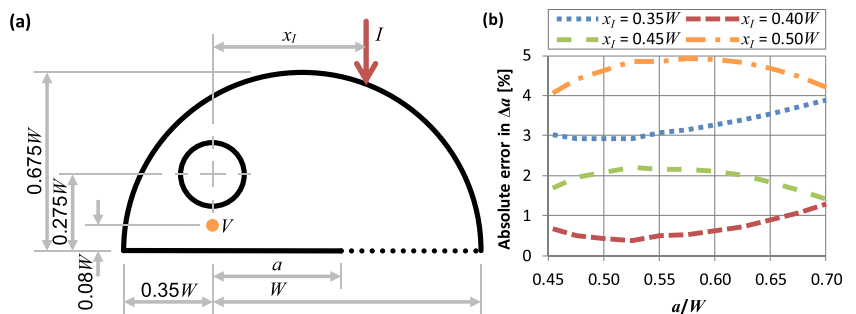
specimen with a large starter notch and a pre-crack of  $0.100 W$  ahead of the notch.

For a C(T) specimen without a starter notch the maximum absolute error in the measurement of crack extension is 2.5% for PD probes across the crack mouth,  $V_{CM}$ , and 7.2% for PD probes along the load-line,  $V_{LL}$ . The addition of the maximum allowable starter notch from ASTM E1820 with a  $0.025 W$  long pre-crack significantly increases these errors. For probe location  $V_{CM}$  it increases to 22.1% whilst for probe location  $V_{LL}$  it increases to 15.7%. If however the length of the pre-crack is extended to  $0.1 W$ , the influence of the notch is much smaller and the maximum error for probe location  $V_{CM}$  becomes 8.3% whilst for probe location  $V_{LL}$  it is 3.6%.

The results of the sensitivity studies demonstrate that the errors associated with the starter notch geometry are much greater than those associated with the application of Johnson’s calibration function. To reduce these errors, the length of the pre-crack ahead of the notch should be at least  $0.1 W$ , consistent with recommendations in a previous investigation [1].

The optimum probe location depends on the starter notch geometry. For a C(T) specimen without a starter notch the optimum location is across the crack mouth but if the specimen includes a starter notch, the optimum location is along the load-line. As discussed above, PD probes along the load-line are also less susceptible to errors associated with large strains around the pin holes. Strain related errors are more likely to occur in a specimen with a starter notch because the amount of

**Fig. 10** (a) DC(T) specimen geometry; (b) corresponding absolute error in the measurement of crack extension for different PD configurations



material between the hole and the notch is greatly reduced. There are, therefore, multiple benefits to locating the PD probes along the load-line in C(T) specimens containing a starter notch.

### CS(T)

The CS(T) specimen geometry considered in this investigation, including the PD configuration, is shown in Fig. 9(a). The PD probes are located across the crack mouth whilst the perpendicular distance between the current injection and the crack plane,  $y_I$ , was varied between  $0.40 W$  and  $0.70 W$  in increments of  $0.10 W$ . The influence of the current injection location on the absolute error in the measurement of crack extension, when determined with Johnson's calibration function, is shown in Fig. 9(b).

The value of  $y_I$  corresponding to the minimum absolute error is  $0.50 W$ . For this PD configuration the maximum absolute error in the measurement of crack extension is 5.4%, however, this error increases significantly if the separation between the current injection points is slightly smaller, e.g. the error increases to 7.4% if  $y_I$  is  $0.40 W$ . To avoid this "cliff-edge" effect, an optimum current injection location,  $y_I$ , of  $0.60 W$  is recommended for CS(T) specimens. For this PD configuration the maximum absolute error in the measurement of crack extension is 5.9%. This error is only slightly higher than the value corresponding to  $y_I = 0.50 W$ , but it is not

significantly sensitive to small, experimental variations in the location of the current injection points.

### DC(T)

The DC(T) specimen geometry considered in this investigation is shown in Fig. 10(a) along with the PD configuration. The PD probe has been located along the load-line whilst the perpendicular distance between the current injection and the load-line,  $x_I$ , was varied between  $0.35 W$  and  $0.50 W$  in increments of  $0.05 W$ . The influence of the current injection location,  $x_I$ , on the absolute error in the measurement of crack extension, when determined with Johnson's calibration function, is shown in Fig. 10(b).

The optimum current injection location,  $x_I$ , considered in this study is  $0.40 W$ . For this PD configuration the maximum absolute error in the measurement of crack extension is 1.3%. This error is not significantly sensitivity to small, experimental variations in the location of the current injection points.

### M(T), DEN(T) & SEN

The M(T), DEN(T) and SEN specimen geometries considered in this study are shown in Fig. 11(a), (b) and (c) respectively, including the PD configurations. Johnson's calibration function is an exact solution for these specimens if the current distribution is uniform but a point current

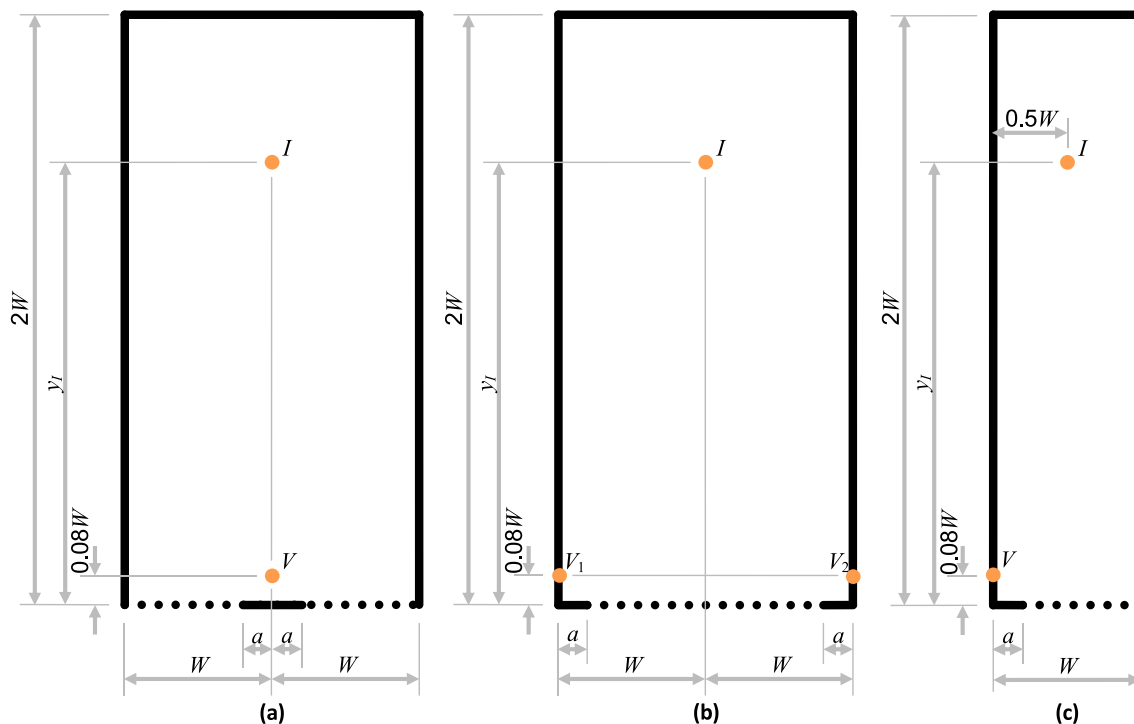
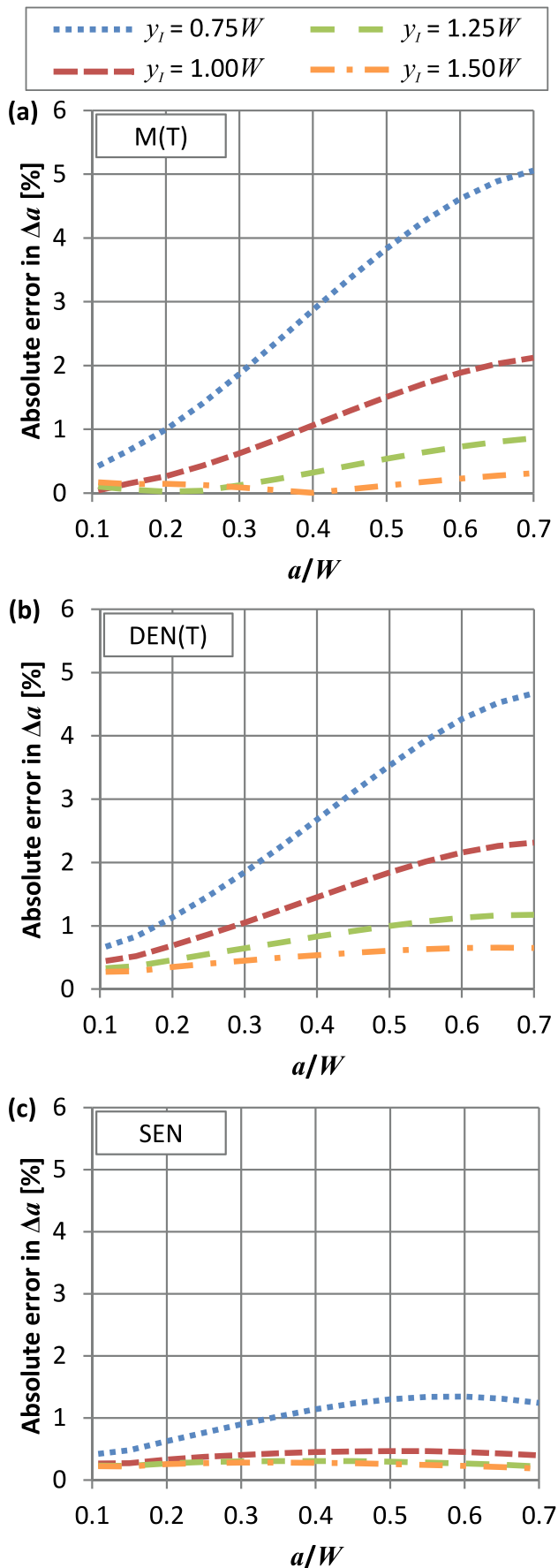


Fig. 11 Specimen geometry for (a) M(T); (b) DEN(T); (c) SEN



◀ Fig. 12 The influence of current injection location on the PD response for a (a) M(T) specimen; (b) DEN(T) specimen; (c) SEN specimen

source has been considered here because it is more representative of most test setups. This will introduce errors in the measurement of crack extension if Johnson's calibration function is applied. As the distance between the crack plane and current injection point,  $y_l$ , increases, the current will tend towards a uniform distribution in the region of the crack, so the error in the measurement of crack extension should reduce. To identify the minimum distance that produces acceptable errors in the measurement of crack extension, the value of  $y_l$  was varied between  $0.75W$  and  $1.50W$  at increments of  $0.25W$ . The influence of the current injection location,  $y_l$ , on the absolute error in the measurement of crack extension is shown in Fig. 12 for M(T), DEN(T) and SEN specimens.

As expected, the absolute error in crack extension reduces as the value of  $y_l$  increases because the current tends towards the uniform distribution assumed in Johnson's calibration function. For M(T) and DEN(T) specimens with a value of  $y_l$  of  $0.75W$ , the maximum error is  $\sim 5\%$ . This error reduces to  $\sim 2\%$  and  $\sim 1\%$  for values of  $y_l$  of  $1.00W$  and  $1.25W$  respectively. For a value of  $y_l$  of  $1.50W$  the maximum error is less than  $1\%$ . The corresponding errors are much smaller for SEN specimens because the increased aspect ratio results in a more uniform current distribution. Based on the results in Fig. 12, a value of  $y_l$  of  $1.25W$  should be sufficient for M(T), DEN(T) and SEN specimens. This is much less onerous than the current guidance in ASTM E647 [2] which suggests a value of  $3.00W$ . For this value of  $y_l$ , the absolute error in the measurement of crack extension is not significantly sensitive to small, experimental variations in the location of the current injection points.

### Unified Calibration Function

The optimised PD configurations for measuring crack extension using Johnson's calibration function, and the corresponding maximum absolute error in the measurement of crack extension, are summarised in Table 1 for the seven most common crack growth specimen types. The results for the starter notch sensitivity study performed on a C(T) specimen are also included. For each of these configurations, the variation in the error in crack extension with crack length is shown in Figs. 13 and 14. Figure 13 corresponds to specimen types that were optimised for  $0.45 \leq a/W \leq 0.70$  and Fig. 14 corresponds to specimen types that were optimised for  $0.10 \leq a/W \leq 0.70$ .

The errors in Table 1, Figs. 13 and 14 are based on the following assumptions:

**Table 1** Maximum error in the measurement of crack extension associated with the application of Johnson's calibration to the optimised PD configurations for the seven most common crack growth specimen types

Specimen Type	Figure	Crack Length Range used for Optimisation	Optimised PD Configuration	Max. error in $\Delta a$ [%]
C(T) (No Starter Notch)	Fig. 6	$0.45 \leq a/W \leq 0.70$	PD probes across crack mouth	2.5
C(T) (Starter notch, 0.1 $W$ pre-crack)	Fig. 6	$0.45 \leq a/W \leq 0.70$	PD probes along load-line	3.6
CS(T)	Fig. 9	$0.10 \leq a/W \leq 0.70$	$y_f = 0.60 W$	5.9
DC(T)	Fig. 10	$0.45 \leq a/W \leq 0.70$	$x_f = 0.40 W$	1.3
M(T)	Fig. 11(a)	$0.10 \leq a/W \leq 0.70$	$y_f = 1.25 W$	0.9
DEN(T)	Fig. 11(b)	$0.10 \leq a/W \leq 0.70$	$y_f = 1.25 W$	1.2
SEN(T)	Fig. 11(c)	$0.10 \leq a/W \leq 0.70$	$y_f = 1.25 W$	0.3
SEN(B)	Fig. 11(c)	$0.45 \leq a/W \leq 0.70$	$y_f = 1.25 W$	0.2

- The PD probes are located  $0.08 W$  from the crack plane (except for the C(T) specimen with a starter notch where they are located as close to the crack plane as possible).
- The specimens do not contain a starter notch, just a pre-crack of infinitesimal width (except for the C(T) specimen with a starter notch).
- The initial crack length,  $a_0$ , is equal to the minimum value in the crack length range used for optimisation (The small differences between the SEN(B) results in Fig. 13 and the SEN(T) results in Fig. 14 are due to the different initial crack lengths).

The maximum absolute error identified in Table 1 is 5.5%, corresponding to the CS(T) specimen. This is relatively small compared to other potential errors associated with the PD technique (for example due to crack tunnelling) which can be  $>25\%$  [1]. Excluding the CS(T) specimen, the maximum absolute error is 3.6%. This corresponds to the C(T) specimen and Johnson's calibration function is already successfully applied to this specimen

type in some standards, e.g. ASTM E1457 [6]. Given this precedent, and the relatively small errors identified in Table 1, it is reasonable to apply Johnson's formula as a single 'unified' calibration function for all seven of the most common crack growth specimen types. Based on the results from the preliminary analyses, this conclusion is applicable to all common specimen thicknesses.

The relationship between crack length and PD is highly dependent on the geometry of any starter notch. This has been demonstrated in previous investigations, e.g. [1], and confirmed by the sensitivity study performed on the C(T) specimen presented above. To avoid a significant increase in the errors presented in Table 1 it is recommended that the length of the pre-crack ahead of any starter notch should be maximised when using Johnson's formula as a single 'unified' calibration function. The minimum permissible pre-crack length should be  $0.1 W$ . A pre-crack of this length can be easily produced by a combination of Electrical Discharge Machining (EDM) and fatigue crack growth.

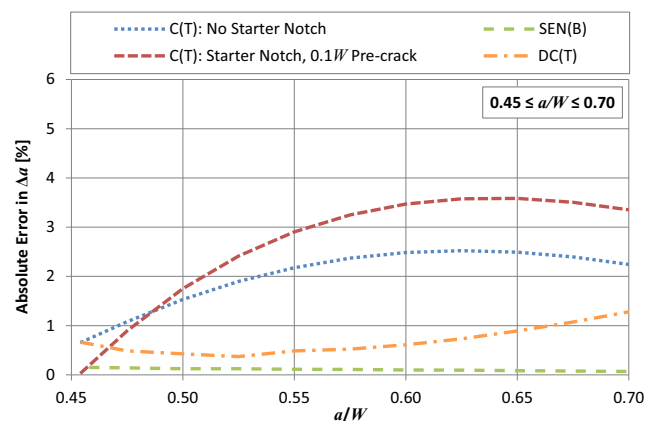


**Fig. 13** Comparison of the absolute error in the measurement of crack extension associated with the use of Johnson's calibration function for the three specimen types optimised for the  $0.45 \leq a/W \leq 0.70$

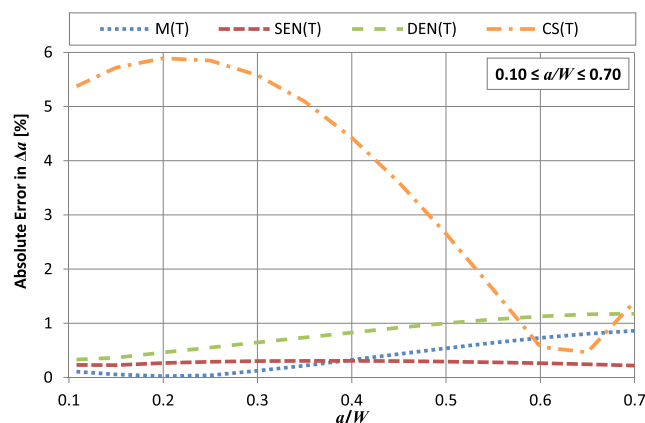


**Fig. 14** Comparison of the absolute error in the measurement of crack extension associated with the use of Johnson's calibration function for the four specimen types optimised for the  $0.10 \leq a/W \leq 0.70$



## Conclusions

Johnson's formula can be used as a single 'unified' calibration function for all seven of the most common crack growth specimen types: C(T), SEN(T), SEN(B), M(T), DEN(T), CS(T) and DC(T). For the exact specimen geometries considered in this investigation, the error in the measurement of crack extension associated with this unified approach is <6%. This is relatively small compared to other sources of error commonly associated with the PD technique. Where the exact specimen geometry cannot be implemented, the following recommendations will ensure that the error remains relatively small:

- The PD probes should be located as close to the plane of the crack as possible.
- The length of the pre-crack ahead of any starter notch should be maximised, with a minimum length of 0.10  $W$ .

**Acknowledgements** The authors would like to acknowledge the Engineering and Physical Sciences Research Council (EPSRC), UK for the support under grant EP/I004351/1. This paper is published with permission of EDF Energy Nuclear Generation Ltd.

**Open Access** This article is distributed under the terms of the Creative Commons Attribution 4.0 International License (<http://creativecommons.org/licenses/by/4.0/>), which permits unrestricted use, distribution, and reproduction in any medium, provided you give appropriate credit to the original author(s) and the source, provide a link to the Creative Commons license, and indicate if changes were made.

## References

1. Tarnowski KM, Nikbin KM, Dean DW, Davies CM (2017) Geometric validity limits for measuring crack growth using the potential drop technique. Submitted to: Eng Fract Mech
2. ASTM E647-15 (2015) Standard test method for measurement of fatigue crack-growth rates
3. Johnson HH (1965) Calibrating the electric potential method for studying slow crack growth. Mater Res Stand 5:442–445
4. Schwalbe K, Hellmann D (1981) Application of the electrical potential method to crack length measurements using Johnson's formula. J Test Eval 9:218–221
5. Tada H, Paris PC, Irwin GR (2000) The stress analysis of cracks handbook, Third edn. American Society of Mechanical Engineers, New York
6. ASTM E1457-15 (2015) Standard test method for measurement of creep crack growth times in metals
7. Gilbey DM, Pearson S (1966) Measurement of the length of a central or edge crack in a sheet of metal by an electrical resistance method. Royal Aircraft Establishment, Farnborough
8. Halliday MD, Beevers CJ (1980) The D. C. Electrical potential method for crack length measurement. In: Beevers CJ (ed) The measurement of crack length and shape during fracture and fatigue. Engineering Materials Advisory Services Ltd., London, pp 85–112
9. Campagnolo A, Meneghetti G, Berto F, Tanaka K (2017) Crack initiation life in notched steel bars under torsional fatigue: synthesis based on the averaged strain energy density approach. Int J Fatigue 100:563–574. <https://doi.org/10.1016/j.ijfatigue.2016.12.022>
10. Aronson G, Ritchie R (1979) Optimization of the electrical potential technique for crack growth monitoring in compact test pieces using finite element analysis. J Test Eval 7:208–215
11. Gandossi L, Summers SA, Taylor NG, Hurst RC, Hulm BJ, Parker JD (2001) The potential drop method for monitoring crack growth in real components subjected to combined fatigue and creep conditions: application of FE techniques for deriving calibration curves. Int J Press Vessel Pip 78:881–891. [https://doi.org/10.1016/S0308-0161\(01\)00103-X](https://doi.org/10.1016/S0308-0161(01)00103-X)
12. Ritchie RO, Bathe KJ (1979) On the calibration of the electrical potential technique for monitoring crack growth using finite element methods. Int J Fract 15:47–55
13. ASTM E1820-15 (2015) Standard test method for measurement of fracture toughness
14. McIntyre P, Priest AH (1971) Measurement of sub-critical flaw growth in stress corrosion, cyclic loading and high temperature creep by the dc electrical resistance technique, report: MG/54/71
15. Ritchie RO, Garrett GG, Knott JP (1971) Crack-growth monitoring: optimisation of the electrical potential technique using an analogue method. Int J Fract Mech 7:462. <https://doi.org/10.1007/BF00189118>
16. COMSOL (2012) Multiphysics v4.3a. Comsol Ltd., Cambridge
17. Tarnowski KM, Dean DW, Nikbin KM, Davies CM (2017) Predicting the influence of strain on crack length measurements performed using the potential drop method. Eng Fract Mech 182: 635–657. <https://doi.org/10.1016/J.ENGFRACMECH.2017.06.008>